Organoindium azides: new precursors to indium nitride

Roland A. Fischer [a,*], Harald Sussek [a], Alexander Miehr [b], Hans Pritzkow [a],
Eberhard Herdtweck [b]

[a] *Anorganisch chemisches Institut der Ruprecht-Karls-Universität, Im Neuenheimer Feld 270, D-69120 Heidelberg, Germany*
[b] *Anorganisch chemisches Institut der Technischen Universität München, Lichtenbergstrasse 4, D-85747 Garching, Germany*

Abstract

The synthesis, properties and the molecular structure in the solid state of triazido(tripyridino)indium (1), the mixed coordination polymer $\{(CF_3SO_3)In[(CH_2)_3NMe_2)]_2(\mu-N_3)In[(CH_2)_3NMe_2)]_2\}_x$ (2) and the polymeric monoazide $\{(N_3)In[(CH_2)_3NMe_2)]_2\}_x$ (3) are reported. Some aspects of the precursor chemistry of 1–3 related to the synthesis of InN thin films are discussed, with special emphasis on the aspect of the accessible chemical purity of the precursors. Compound 3 allowed the growth of crystalline InN thin films at 300–450°C in the absence of ammonia using the technique of organometallic chemical vapor deposition. © 1997 Elsevier Science B.V.

Keywords: Indium; Azides; Indium nitride; MOCVD; Thin films

1. Introduction

Since the development of the first optoelectronic solid state devices about 25 years ago there has been a continuous demand for efficient blue and UV light emitting materials. The group-13 nitrides are the most potent materials for this purpose. The wide direct band gap (1.9 eV InN; 3.45 eV GaN; 6.2 eV AlN), their isomorphous miscibility allowing band gap engineering as well as other materials properties including inertness, mechanical hardness and high thermal stability, radiation resistance, large avalanche breakdown fields and large high-field electron drift velocities, makes the Al-GaInN quaternary alloy system uniquely suited for numerous device applications [1]. Because of the large equilibrium dissociation pressure of nitrogen over the nitrides at typical growth temperatures (e.g. 10^5 atm at 1100 K for InN) it is not feasible to grow large single crystals from the melt like in the case of silicon or the other III/V semiconductors, e.g. GaAs. To date, vapor phase heteroepitaxy of the materials on single crystalline substrates is the only method to fabricate device quality crystalline group-13 nitride materials. All com-

mercial available devices are grown by organometallic vapor phase epitaxy (OMVPE [2]) using trialkyl derivatives of the group-13 metals and ammonia as reagents. High output at comparably low costs are the main advantages of OMVPE over physical methods like MBE [3]. The growth of the nitrides by thermal methods necessitates minimum substrate temperatures above 550°C to activate ammonia. Typical deposition temperatures for AlN and GaN are above 950°C, which is in the range of the decomposition temperatures of the respective nitrides [4]. Mainly for this reason the ammonia to group-13 component ratio is very large ($> 10^3$) during the OMVPE process. As a consequence, the hydrogen incorporation into the grown nitride thin films is high and the OMVCD grown materials are difficult to p-dope. Especially the growth of InN or indium-rich ternary phases is a severe problem. Because of the low decomposition onset ($\sim 600°C$) of InN [4] the formation of indium droplets on the surface of the InN layer occurs. The authors of a very recent review article on the properties and growth of group-13 nitrides state in their summary: The most pressing need is for an InN precursor which deposits high-quality InN at growth temperatures less than 500°C and allows higher indium mole fractions to be incorporated in device quality ternary and quaternary alloys with gallium and aluminum nitrides. [1].

---

* Corresponding author. Fax: +49 6221 546617; e-mail: roland.fisher@urz.uni-heidelberg.de

2. Growing the nitrides from single sources: a simple, elegant solution for a complex problem?

For certain examples it was demonstrated that the use of single molecule precursors rather than applying two independent sources allows elegant molecular control over the composition of binary thin films leading to stoichiometric growth even with simple equipment [5]. In the case of the group-13 nitrides, the incorporation of the nitrogen in a chemically activated form into the precursor compound may lead to stoichiometric growth in the absence of ammonia at much lower temperatures as compared to the conventional methods. An ideal single source precursor for InN would be a non-pyrophoric, non-explosive, non-toxic, air-stable liquid compound with a high vapor pressure (> 1 Torr at moderate conditions), exhibiting a molecular structure with strong covalent In–N bonds and no or at least only few In–C, C–C, C–H, N–C or N–H bonds and no other types of chemical bonds. To ensure stoichiometric growth the precursor should be nitrogen rich and the thermal stabil-

ity of the compound should be comparably low (dec. ~ 250°C). Unfortunately, the known compound triazidoindium, $In(N_3)_3$, which meets most of the above criteria, is explosive and a non-volatile solid [6]. Already some years ago in 1989, namely Beach et al. [7] and Gladfelter et al. [8] demonstrated the potential of organometallic derivatives of the parent triazides $E(N_3)_3$, e.g. $[R_2E(N_3)]_3$, for the growth of the nitrides EN (E = Al, Ga). The fragmentation of the azide group into dinitrogen and a reactive nitrene intermediate is a well known decomposition pathway of covalent azides [9,10]. Against this background, the chemistry of group-13 azides in general has still remained rather undeveloped. Since the early work of Wiberg et al. in the mid 1950s and the contributions of Dehnicke et al. in the late 1960s (see Table 1) it was only quite recently when Cowley et al. [11] and ourselves [12–16] independently started out to study the coordination chemistry of group-13 azides in more detail, aiming at novel and improved precursor compounds for OMVPE of the nitrides. Lately we communicated our preliminary results on the appli-

Table 1
Review of known azide compounds of aluminium, gallium and indium (structurally characterized compounds are represented in *italics*)

|	Aluminium	Gallium	Indium
Monoazides	$X_2Ga(N_3)$; X = Br, I [m]	*[Me₂GaN₃]ₙ* [b]	$(CH_3)_2In(N_3)$ [g]
	$K[(Me_2Al)_2N_3]$ [o]	*[(R₃N)₃Ga(η¹-N₃)]₂* [c]	$(C_2H_5)_2In(N_3)$ [h]
	$(R_2)Al(N_3)$ [p]	$Et_2Ga(\mu-NH_2)(\mu-N_1)GaEt_2$ [a]	$(C_4H_9)_2In(N_3)$ [k]
	$[(CH_3)_3NMe_2]Al(N_3)$ [a]	$[(CH_3)_3NMe_2]Ga(N_3)(Do)$ Do = ClI₃, 'Bu [a]	$[(CH_3)_3NMe_2]_2In(N_3)$ [l]
	$[Me_2(H_2N'Bu)Al(N_3)$ [a]	*(Octaethylporphyrinato-N,N,N,N)Ga(N₃)* [d]	
		$X_2Ga(N_3)$; X = Br, I [m]	
Diazides	$Me_3N[Me_2Al(N_3)_2]$ [n]	*[2,6-(Me₂NCH₂)₂C₆H₃]Ga(N₃)₂* [c]	
	$(R)Al(N_3)_2$ [p]	$Me_2N[Me_2Ga(N_3)_2]$ [n]	
		$EtGa(N_3)_2$ [a]	
		$(Et)(N_3)_2Ga(Do)$;	
		Do = THF, H₂N'Bu, Py, NC₇H₁₃ [a]	
		$Cp(CO)_3W-Ga(N_3)_2(NMe_3)$ [a]	
		$Cp(CO)_2Fe-Ga(N_3)_2(Py)$ [a]	
		$(CO)_4Co-Ga(N_3)_2(NMe_3)$ [a]	
Triazides	$[Al(N_3)_3]_x$ [f]	$[Ga(N_3)_3]_x$ [i]	$[In(N_3)_3]_x$ [i]
	(py)₃Al(N₃)₃ [s,t]	*(Et₃N)Ga(N₃)₃* [a]	*(py)₃In(N₃)₃* [t]
	$\{[(thf)_2Na][(thf)_2Al(N_3)_4]\}_x$ [t]	$(Me_3N)Ga(N_3)_3$ [a]	$\{[(py)_2Na][(py)_2In(N_3)_4]\}_x$ [t]
		$(H_{11}C_7N)Ga(N_3)_3$ [a]	
		(py)₃Ga(N₃)₃ [a,r]	
		$(TMEDA)_3[Ga(N_3)_4]_2$ [a]	
		$(1,4,7-Trimethyl-1,4,7-triaza-cyclononan)Ga(N_3)_3$ [a]	
		$(PMDT)Ga(N_3)_3$ [a]	
		$Li(CH_3)Ga(N_3)_3$ [a]	

[a] A. Miehr, Dissertation, Technische Universität München, 1996. [b] D.A. Atwood, R.A. Jones, A.H. Cowley, J.L. Atwood, S.G. Bott, J. Organomet. Chem. 394 (1990) C6. [c] D.A. Neumayer, A.H.Cowley, A. Decken, R.A. Jones, V. Lakhotia, J.G. Ekerdt, J. Am. Chem. Soc. 117 (1995) 5893. [d] A. Coutsolelos, R. Guilard, A. Boukhris, C. Lecomte, J. Chem. Soc. Dalton Trans. (1986) 1779. [e] A.H. Cowley, F.P. Gabbai, F. Olbrich, S. Corbelin, R.J. Lagow, J. Organomet. Chem. 487 (1995) C5. [f] E. Wiberg, H. Michaud, Z. Naturforsch. 9B (1954) 495–497, 502–503. [g] N. Röder, K. Dehnicke, Chimia (Switz.) 28 (1974) 349–351. [h] J. Müller, K. Dehnicke, J. Organomet. Chem. 12 (1968) 37–47. [k] T.N. Srivastava, K. Kapoov, Ind. J. Chem. A 17 (1979) 611–612. [l] R.A. Fischer, A. Miehr, T. Metzger, E. Born, O. Ambacher, H. Angerer, R. Dimitrov, Chem. Mater. 7 (7) (1996) 1356–1359. [m] K. Dehnicke, N. Krüger, Z. Anorg. Allg. Chem. 444 (1978) 71. [n] K. Dehnicke, N. Röder, J. Organomet. Chem. 86 (1975) 335. [o] J.L. Atwood, W.R. Newberry, J. Organomet. Chem. 87 (1975) 1. [p] J.S. Thayer, J. Organomet. Chem. Rev. 1 (1966) 157; M.I. Price, J. Organomet. Chem. 5 (1966) 584; K. Dehnicke, J. Strahle, D. Seybold, J. Müller, J. Organomet. Chem. 6 (1966) 298; V. Krieg, J. Weidlein, Z. Anorg. Allg. Chem. 368 (1969) 44. [r] C.J. Carmalt, A.H. Cowley, R.D. Culp, R.A. Jones, J. Chem. Soc. Chem. Commun. (1996) 1453. [s] R.A. Fischer, A. Miehr, H. Sussek, H. Pritzkow, E. Herdtweck, J. Müller, O. Ambacher, T. Metzger, Chem. Commun. (1996) 2685. [t] H. Sussek, Diploma Thesis, Ruprecht-Karls-Universität Heidelberg, 1996.

cation of a new organometallic InN single molecule precursor [17]. Here we wish to present our results on the synthesis and structural chemistry of novel indium azides, which are of interest as precursors for InN.

3. Synthesis and properties

According to Wiberg et al. the triazides $E(N_3)_3$ are accessible by the treatment of ECl_3 in THF solution with sodium azide (Scheme 1). The primary products are the soluble species $(THF)_nE(N_3)_3$ which can be separated by filtration. These intermediates easily lose the coordinated solvent and the highly explosive triazides $E(N_3)_3$ are obtained. However, such samples are always contaminated by traces of NaCl and excess NaN_3 (checked by elemental analysis and XRD). In addition, the reaction is complicated by the formation of highly associated insoluble tetraazido complexes, which we have structurally characterized [18] and will be reported elsewhere. For gallium it was shown previously, that by using suitable donor ligands it is possible to break up the polymeric structure of $Ga(N_3)_3$. Some examples of the resulting monomolecular Lewis-base adducts $(L)_nGa(N_3)_3$ have been characterized analytically and spectroscopically [13,14]. A single crystal X-ray diffraction study of $(py)_3Ga(N_3)_3$ revealed the expected octahedral structure with a meridional arrangement of the terminal azide groups [14]. Parallel to our work Cowley et al. communicated a different multi-step

synthesis and structural data on $(py)_3Ga(N_3)_3$, too [19]. Aiming at ultra high purity of the potential new precursors for nitride growth, special reagents and multistep synthesis clearly represent a problem. Also, the use of ethers as solvents should be avoided as far as possible. The cleavage of the C–O bond at Lewis-acidic centers may occur at least in traces. This mechanism may lead to unacceptably high levels of O-impurities in the precursors. The grown GaN films will then be intrinsically contaminated with traces of oxygen, giving rise to unwanted characteristic photoluminescence at 3.37 eV [12]. It is thus far more elegant to synthesize the key compounds $(py)_3E(N_3)_3$ (or similar amine stabilized derivatives [13]) in a one-step reaction directly from EX_3 (X = halide) and stoichiometric amounts of sodium azide in amines, e.g. pyridine, as solvents. The yields are quantitative and the reagents are available in high purity. The vapor pressures of the Lewis-base adducts $(L)_nE(N_3)_3$ studied so far are too low to give reasonable growth rates in OMCVD experiments, which have to be about 1 nm s^{-1}. But the growth of polycrystalline GaN thin films using spin-on pyrolysis methods is possible [15]. By introduction of a hydrocarbon ligand capable of intramolecular adduct formation and thus sacrificing one or two of the azido groups, fairly volatile monomeric (gas phase) organometallic group-13 azide precursors are accessible. These derivatives are not explosive. They are also non-pyrophoric and only moderately moisture sensitive. Interestingly, the indium compound 3 is air stable and does not react with ammonia even in the
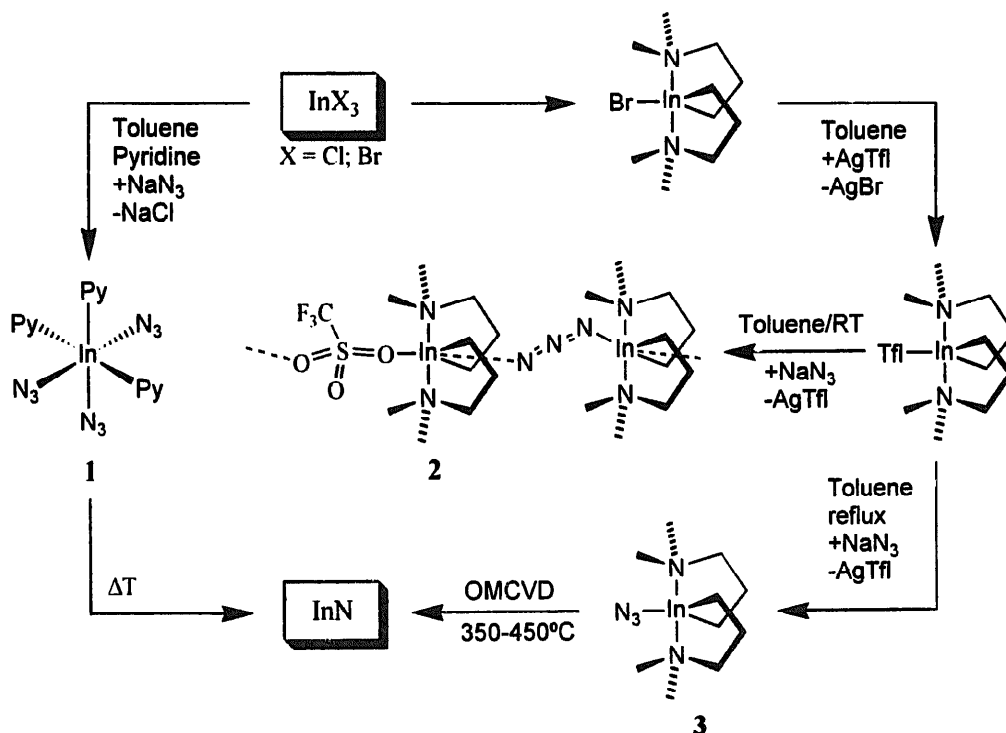
Scheme 1. Synthetic routes to compounds 1, 2 and 3.

melt. Schumann et al. have shown that related intramolecularly adduct stabilized group-13 metal alkyls also exhibit advantageous properties as novel precursors for OMVPE of GaAs and InP [20]. Especially oxygen incorporation is suppressed by using intramolecularly adduct stabilized group-13 metal precursors [21]. An optimized synthetic route still remains to be worked out which allows to obtain precursors such as 3 by a one pot synthesis via intermediates of type 1 in amines as solvents. For gallium recent results confirm this possibility [15]. For aluminium [16] and indium only stepwise routes were successful, so far. In the case of indium the exchange of the halide substituent by a better leaving group ($CF_3SO_3^-$, PF_6^-) proved to be necessary (Scheme 1). If the excess of sodium azide and the temperature are too low and/or the reaction time is to short, the intermediate 2 is more or less abundant in the reaction mixture and cannot be quantitatively separated by crystallization or sublimation from the product 3. Halide bridged species similar to 3 can be expected to be present as impurity for the same reasons. Then, the analytical data of the recrystallized and sublimed products (!) show values of halide (or S. which comes from the triflate) in the range between 1–10 wt%.
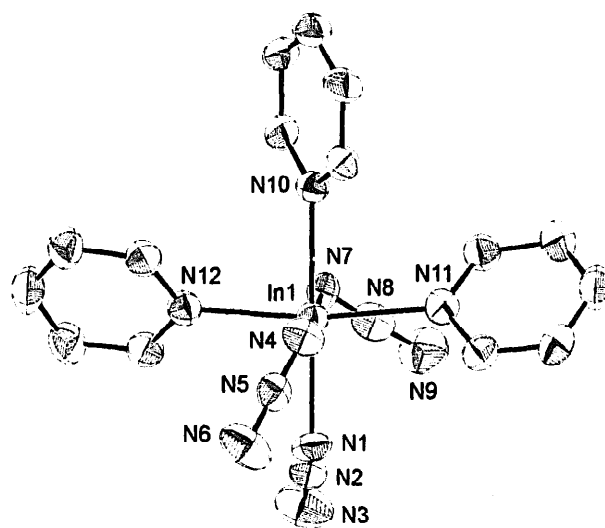
4. Structure

4.1. Molecular structure of 1

The compound crystallizes from toluene/pyridine solvent mixtures as colorless large plates in the triclinic space group P1̄. The monomeric molecular units in the crystal (Fig. 1). show no noticeably short intermolecular contacts. The indium center is coordinated octahedrally with the azide groups arranged meridionally. The angles $In-N_\alpha-N_\beta$ and $N_\alpha-N_\beta-N_\gamma$ are reasonably close to the "ideal" values of 120° and 180° of covalently bonded azides. Compound 1 is thus isostructural to the previously reported homologs of aluminium and gallium. However, it is necessary to compare some of the structural details within this homologous series. A typical feature of covalent azides is the alternation of the N–N bond lengths [9]. The $N_\alpha-N_\beta$ bond is long and the $N_\beta-N_\gamma$ bond is shorter (for example: BrN_3: 123 and 113 pm [9]; $\Delta(N-N) = 10$ pm). In accordance with NBO analysis [9] this can be interpreted as the solid state manifestation of the classical Lewis representation of covalent azides with two non-bonding electron pairs at the N_α and a formal triple bond between N_β and N_γ. For the aluminium and gallium complexes the azide groups trans to each clearly exhibit this feature with a value of $\Delta(N-N) = 5 \pm 1$ pm [14,16]. For indium the alternation of the respective N–N distances is small (< 2 pm) and close to error of the structure determination. This agrees with a more ionic description of the

Fig. 1. Molecular structure of 1 in the solid state (ORTEP-plot with 50% probability thermal ellipsoids). Selected distances (pm) and angels (°): In–N1 223.5(2), In–N4 219.3(2), In–N7 223.3(2), In–N11 (231.1(2), In–N10 229.9(2), In–N12 227.9(2), N4–N5 116.6(3), N5–N6 117.1(3), N7–N8 115.6(3), N8–N9 117.3(4), N1–N2 106.0(4), N2–N3 121.3(4); N4–In–N1 89.99(9), N4–In–N7 176.68(8), N4–In–N11 88.52(9), N4–In–N10 85.40(8), N4–In–N12 91.05(9), N1–In–N7 93.10(9), N1–In–N10 175.39(8), N7–In–N11 89.99(8), N7–In–N10 91.50(8), N7–In–N12 89.96(9), N11–In–N10 84.01(8), N11–In–N12 171.10(7), N4–N5–N6 176.0(3).

$In-N_{azide}$ bonds. A striking common feature of the aluminum and indium complexes in contrast to the gallium compound [12–16,19] should be mentioned. The N–N distances of the azide group in trans position to one pyridine ligand are unusual, the $N_\alpha-N_\beta$ is short and the $N_\beta-N_\gamma$ bond is longer (Fig. 1)! This and the general small non-systematic variation of $E-N_{azide}$ and $E-N_{py}$ distances, which resulted in case of the Al and In compounds (Fig. 1) but not for the gallium complex, could be an effect in the solid state and the structural details should not be overestimated in these cases.

4.2. Molecular structure of 2

Compound 2 crystallizes as colorless needles from toluene/n-pentane in the monoclinic space group $P2_1/n$. In the solid state compound 2 forms one-dimensional polymeric chains. The chain structure is built up by alternating head to tail bridging azide and triflate groups. Fig. 2 shows the repeat unit of the structure. The structure can be interpreted as the co-crystallization of two different monomeric species $(CF_3SO_3)In[(CH_2)_3NMe_2]_2$ and $(N_3)In[(CH_2)_3NMe_2]_2$. In the solid state both nitrogen atoms are coordinated at the indium centers. The bridging azide group exhibits significantly different distances between the terminal N atoms and the indium centers. In1–N3 amounts to 230.9 pm and In2–N5 with 256.4 pm is longer. The shorter distance compares to the
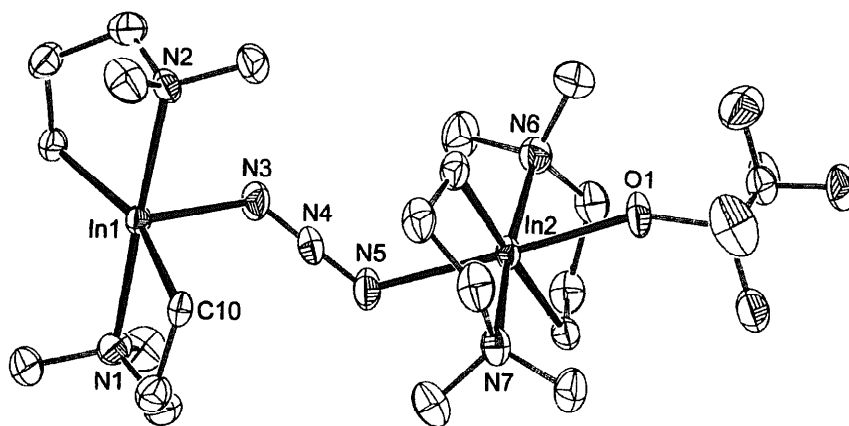
Fig. 2. Molecular structure of **2** in the solid state (ORTEP-plot with 50% probability thermal ellipsoids). Selected distances (pm) and angels (°):
In1–N1 248.9(3), In1–N2 248.8(3), In1–N3 230.9(3), In1–C5 214.9(4), In1–C10 215.0(3), N3–N4 118.4(4), N4–N5 116.6(4), In2–N5 256.4(3),
In2–N6 249.8(3), In2–N7 249.9(3), In2–C15 214.5(4), In2–C20 214.3(4), In2–O1 247.3(2), N1–In1–N2 173.84(10), N1–In1–N3 86.90(11),
N2–In1–N3 88.37(11), N3–In1–C5 100.76(14), N3–In–C10 100.79(15), C5–In1–C10 158.15(14), In1–N3–N4 126.3(3), N3–N4–N5 177.7(4),
N4–N5–In2 123.2(2), N5–In2–N6 93.84(11), N5–In2–N7 92.64(11), N5–In2–O1 175.49(9), N6–In2–N7 173.49 (10), N6–In2–C15 79.92(13),
N6–In2–C20 99.14(14), N7–In2–C15 100.38(13), N7–In2–C20 80.41(14).

In–N$_{azide}$ covalent bond similar to **1**. The longer distance reflects the weaker dative donor acceptor type bond to an adjacent In center. The angles In1–N3–N4 of 126.2° and N4–N5–In2 of 123.3° are within the expected range and again correspond to the sp^2 hybridization of the N atoms. A similar situation is found for the coordination of the triflate group. The indium oxygen bond distances range from 247.3 pm (In2–O1) to 309.2 pm (In1–O2). The best description of the structure of **2** is that of an infinite association of the dimeric unit {(CF₃SO₃)In[(CH₂)₃NMe₂)]₂(μ-N₃)In[(CH₂)₃NMe₂)]₂}, with a hexacoordinated center In2 and a pentacoordinated center In1. This latter In atom is weakly coordinated to an O atom of the next triflate group. Similarly ordered, polymeric structures

have already been described by Schumann et al. for Br–In[(CH₂)₃NMe₂)]₂ and I–In[(CH₂)₃NMe₂)]₂ as well as by Cowley et al. for related indium halides [22]. The In1 atom rests in the center of a distorted trigonal bipyramid. The nitrogen atoms of the chelating ligands are at the axial positions (N1–In1–N2 173.87°). The weak coordination of the oxygen atom O2 of the triflate group causes a characteristic widening of the angle C5–In1–C10 to 158.1° from the ideal value of 120° expected for a trigonal bipyramidal structure. The coordination of the In2 center is clearly closer to an octahedral geometry. The distances In2–N5, In2–O1, In2–N6 and In2–N7 are quite similar ranging around 250(±6) pm, while the In2–C20 and In2–C16 bond lengths of about 214 pm are much shorter. The angles C20–In2–

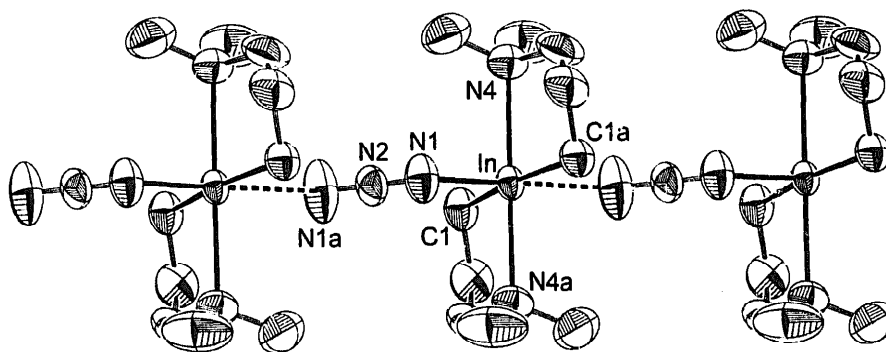
Fig. 3. Molecular structure of **3** in the solid state (ORTEP-plot with 50% probability thermal ellipsoids). Selected distances (pm) and angels (°):
In–N1 252.6(2), In–N4 249.6(2), In–C1 214.8(2), N1–N2 116.5(2), N1–In–N4 88.94(8), N1–In1–N4a 91.06(8), N1–In–C1 91.11(8),
N1–In–C1a 88.89(8), C1–In–C1a 180.00, N4–In–N4a 180.00, N4–In–C1 80.12(8), N4a–In–C1 99.88(8), N1–N2–N1a 180.0, In–N1–N2
119.44(14).

C15, N6–In2–N7 and N5–In2–O1 are all close to 180°. The atoms C20, N7, In2, N6 and C15 are almost coplanar.

4.3. Molecular structure of 3

Compound 3 crystallizes as colorless needles from CH_2Cl_2/n-pentane solutions at $-30°C$ in the triclinic space group P$\bar{1}$. The solid state structure of 3 (Fig. 3) again shows one-dimensional polymeric chains. The head to tail bridging mode of the azide moiety is similar to compound 2. However, N2 and In are both centers of symmetry now. Therefore there is only one characteristic In–N$_{azide}$ bond for the infinite chain: In–N1 of 252.6 pm and the bridging azide unit is symmetric also, e.g. N1–N2 = 116.5 pm. It should be noted, that the homologous Al compound $(N_3)Al[(CH_2)_3NMe_2]_2$ is monomeric in the solid state without noticeably short intermolecular Al–N$_{azide}$ contacts [16]. The respective Ga homologue is currently under investigation. The bonding parameters of the azide groups of the almost octahedrally coordinated In center compare well with compounds 1 and 2 respectively. Because of symmetry, the angles N4–In–N4a, N1–In–N1a and C1–In–C1a are now exactly 180° and the In centers are no longer chiral as it was the case for 2. Compound 3 shows an interesting phase transition. Both forms, the high temperature form and the low temperature form are triclinic P$\bar{1}$. At temperatures higher than $-30°C$ the symmetry of the molecular structure reduces, N2 and In are no longer inversion centers and the In–N$_{azide}$ distances alternate in the same way as it is observed for 2. This transition goes along with an extension of the unit cell. A detailed crystallographic analysis of this behavior will be published elsewhere [23].

5. Thin film growth

5.1. Stoichiometric crystalline InN films

Using a horizontal isothermal hot walled tube reactor [24] at temperatures from 300 to 500°C quite pure (EDS, Fig. 4; carbon and oxygen impurities are below the detection limit of 0.5 at%) and crystalline InN films (Fig. 5) were deposited from precursor 3 on (111) silicon, (001) GaAs and (0001) Al_2O_3 (sapphire, also with AlN and GaN buffer layers) substrates. Various conditions were employed, either without any carrier gas in vacuo or using a mixture of N_2 and NH_3 as carrier gases. The growth rates (by profilometry) were between 0.3 μm/h (best crystallographic properties) up to 5 μm/h (homogeneous, very smooth surface, polycrystalline or amorphous nature). The main constituents (> 95%) of the exhaust gases (GC/MS; NMR spectroscopy of the condensables) were unsaturated amines
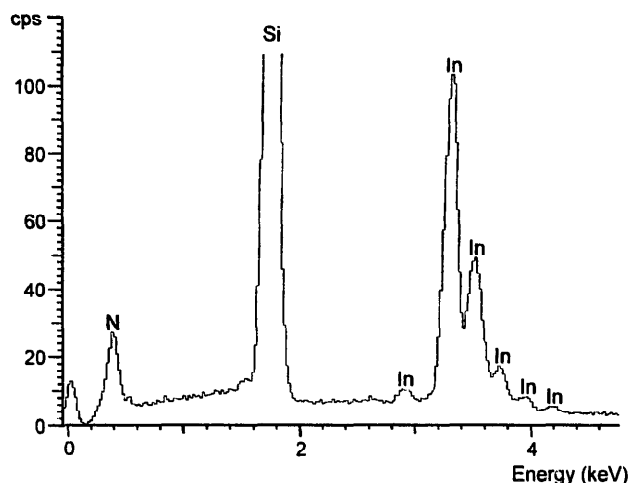

Fig. 4. EDX spectra of a crystalline InN film deposited from compound 3 by OMCVD.

e.g. $H_2C=CHCH_2NMe_2$. Thus, the nitrogen atom of the chelate ring of 3 does not serve as the (major) N source for the InN growth. X-ray diffraction studies on representative samples revealed the common hexagonal wurtzite phase of InN and the preferred orientation of the (002) direction of the InN crystallites parallel to the (001) direction of single crystalline sapphire substrate.

5.2. Effect of impurities

The precursor chemistry of thin films represents a rather flourishing branch of organometallic chemistry. But there is one aspect of this chemistry which appears to be faded out almost constantly in the published literature. It deals with the purity and the chemical log-term stability of the proposed novel precursors. This is by no means a trivial question [25]. New organometallic compounds are usually obtained in chemical purities less than 99%. The reported analytical data are mostly incomplete. And in addition it is often very difficult to identify the chemical nature of the
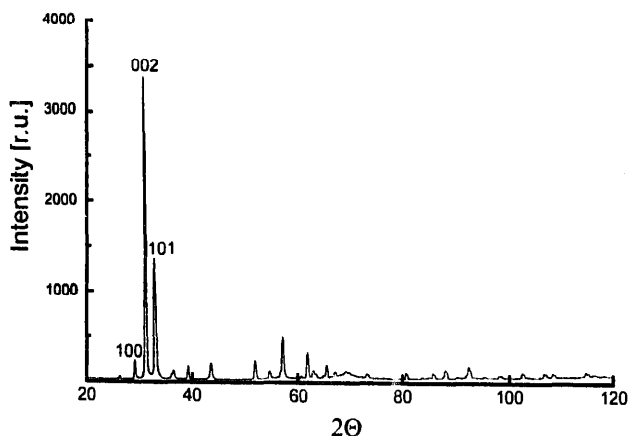

Fig. 5. XRD pattern of a crystalline InN film deposited from precursor 3 by OMCVD.

impurities. However, the properties of thin films grown from new precursors may very well be strongly affected by such impurities. In certain cases it may be difficult to tell which results depend on intrinsic chemical features of the precursor and which are caused by probably overlooked impurities as well as by the conditions of the deposition experiment (e.g. leaking). In the case of semiconducting materials, such impurities clearly represent an important issue, when novel precursors are discussed.

5.2.1. Metallic indium

As mentioned in Section 1, the growth of stoichiometric InN by classical methods represents a problem, due to the low lying decomposition onset of InN. Also, our vacuum deposition experiments at higher substrate temperatures (> 500°C) expectedly resulted in somewhat N-deficient films, due to incipient decomposition of InN [4]. This is indicated by the occurrence of characteristic reflections of elemental In in the XRD patterns of those films (e.g. the 100 and 002 reflections of In metal; see Fig. 6). The reason for the occasional occurrence of metallic indium of some films at deposition temperatures as low as 300°C, however, proved to be quite different. Trace amounts of the starting material $BrIn[(CH_2)_3NMe_2)]_2$ (~ 0.1–5 mol%) can be present as impurity of the precursor, which is difficult to remove by recrystallization and sublimation. This is probably due to the formation of stable mixed azide/halide coordination polymers similar to 2, which issue has been discussed earlier. This impurity however decomposes cleanly into In, InBr and $InBr_3$ under the conditions of the OMCVD experiment, as indicated by thin yellow to orange coatings of the reactor wall at the cooler parts of the reactor exit and traces of a white residue collected in the cold trap. These materials were identified as InBr and $InBr_3$ respectively (EI-MS, elemental analysis). As shown by EDS, the films were free of Br (i.e. Br < 0.1 at%, detection limit). Thus, the observed metallic indium (by XRD) in some of our low temperature experiments is in fact excess In! It comes from the decomposition of traces of $BrIn[(CH_2)_3NMe_2)]_2$ or $CF_3SO_3In[(CH_2)_3NMe_2)]_2$ rather than decomposition of grown InN.

5.2.2. Indium oxide

In the case of controlled leaking or impure carrier gases, e.g. ammonia, the grown films were contaminated with the cubic In_2O_3 phase. Although precursor 3 is very stable against moisture and oxygen at ambient conditions, the formation of In_2O_3 at elevated temperatures even in the presence of excess ammonia is fully understandable by the comparison of the heat of formation of InN (34 kcal/mol) [26] and In_2O_3 (221 kcal/mol) [27]. Using high purity ammonia (99.999%) oxygen contaminations detectable by XRD were absent.
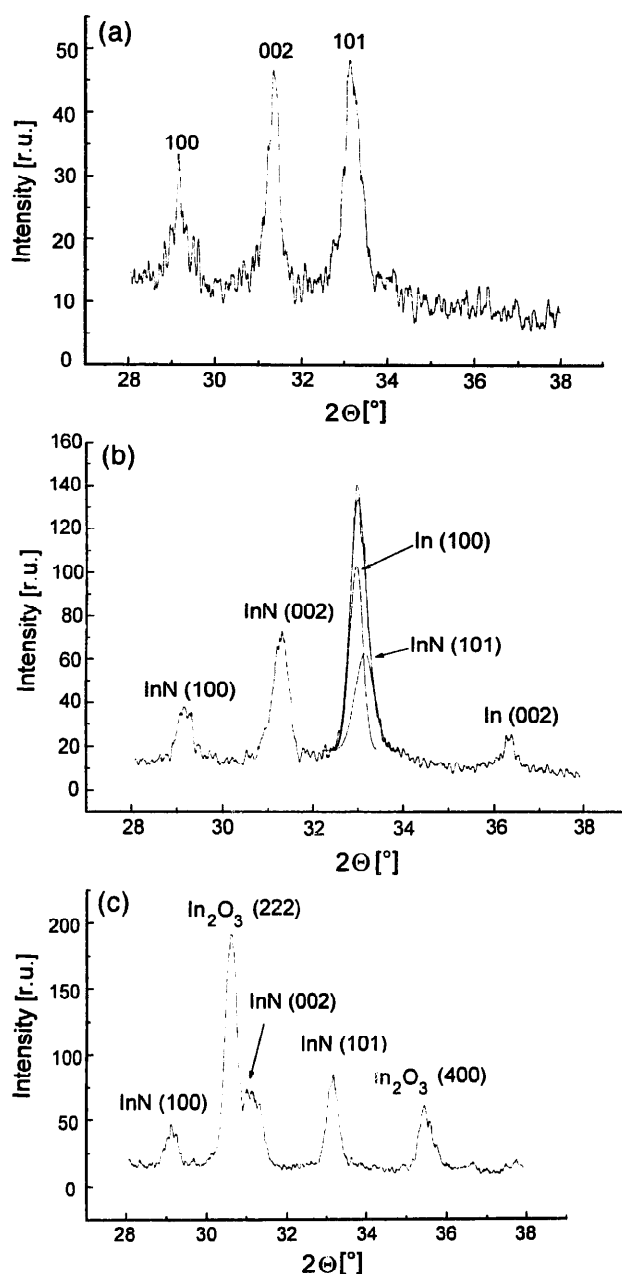

Fig. 6. XRD patterns of various InN thin films grown by OMCVD using precursor 3. (a) "pure" InN thin film (see Fig. 5); (b) formation of metallic indium; (c) formation of cubic indiumnitride.

Films grown with the purified precursor (> 99.9%, by elemental analysis) under vacuum conditions showed no metallic In by XRD (LPOMCVD experiments at 450°C; no NH_3 added).

The important conclusion is, that the composition of the deposited InN layers at temperatures below 500°C depends only on the chemical purity of the precursor compound and the reaction conditions and not on intrinsic structural or chemical features of the precursor molecule. The InN films may still contain some amounts of other impurities (e.g. Si, Cl, Li, etc.; introduced by the chemical synthesis of 1, but were not detectable by means of EDS and XPS).

6. Conclusions

The first examples of structurally characterized indium azides were reported. Compound **3** serves as the first low temperature single source precursor to grow stoichiometric and crystalline InN by OMCVD. Future work has to concentrate on an optimized synthetic strategy to obtain intramolecularly adduct stabilized organometallic indium azides similar to **3** in electronic grade purity. The triazides $In(N_3)_3$ and its Lewis-base adducts like $py_3In(N_3)_3$ may serve as key compounds for this purpose.

7. Experimental

7.1. General procedures

All manipulations were performed utilizing carefully dried reaction vessels (Schlenk techniques) under an inert atmosphere of purified argon and so far as required by using the glove box. Solvents were dried under N_2 by standard methods and stored over 4 Å molecular sieves (residual water < 3 ppm, Karl-Fischer). The ^1H and ^{13}C NMR spectra recorded on a Jeol JNM 400-GX and a Bruker EM 200 were referenced to residual protic impurities of the internal solvent and corrected to tetramethylsilane. The IR spectra were obtained in solution (toluene, pyridine) using 0.1 mm CaF_2 and NaCl cells on a Perkin Elmer 1650 FT IR or a Bruker IFS 66. Elemental analysis were provided by the Microanalytical Laboratories of the Technical University at Munich and of the Chemical Institute of the University of Heidelberg.

7.2. Synthesis of $(py)_3In(N_3)_3$ (1)

A suspension of 1.02 g (4.16 mmol) of dry indium(III)chloride and 0.94 g (14.48 mmol) of sodiumazide in 20 mL toluene was refluxed for 5 h. After cooling down to $-78°C$ a solution of 30 mL pyridine in 30 mL toluene was added and refluxed for an additional 15 h. After filtration the solvent was removed in vacuo remaining colorless, well developed crystals. Yield 0.95 g (1.98 mmol); 47.59%. Melting point 237°C. Anal. Found: C, 37.73; H, 3.41; N 32.90; In, 23.20. $C_{15}H_{15}InN_{12}$ ($M = 478.19$). Calc.: C, 37.67; H, 3.16; N, 35.14; In, 24.01. IR (pyridine, NaCl, cm^{-1}): 2084 vs; 2068 vs; 2055 sh; (N_3 asym.). The sample explodes uncontrolled upon fast heating around 300°C.

7.3. Synthesis of $[(N_3)In[(CH_2)_3NMe_2]_2(CF_3SO_3)In-[(CH_2)_3NMe_2]$ (2)

A solution of 0.528 g (1.44 mmol) $BrIn[(CH_2)_3NMe_2]_2$ [28] in CH_2Cl_2 was added to 0.37

g (1.44 mmol) $Ag[CF_3SO_3]$ and refluxed for 48 h. After filtration, removing the solvent, and dissolving the residue in toluene, the solution was added by filtration to a suspension of 0.1 g (1.53 mmol) of dried sodium azide in toluene. The mixture was warmed up to 100°C for 2 h. Analytically pure colorless needlelike crystals were obtained by filtration, removing the solvent and recrystallization from toluene/n-pentane. Yield 1.0 g (1.3 mmol; > 90%). Anal. Found: C, 33.02; H, 6.13; N 13.09. $C_{21}H_{48}N_7In_2O_3F_3S$ ($M = 765.35$). Calc.: C, 32.96; H, 6.32; N, 12.18. ^1H NMR (benzene-d_6, 25°C) $\delta = 0.53$ (t, 2H, $InCH_2$); 1.56 (quin, 2H, $-CH_2-$); 1.82 (t, 2H, NCH_2); 1.91 (s, wide, 6H, NCH_3). IR (toluene, CaF_2, cm^{-1}): 2158 vs (N_3, asym.); 1462 s (N_3, sym.).

7.4. Synthesis of $[(CH_2)_3NMe_2]_2In N_3$ (3)

A solution of 6.685 g (18.2 mmol) $BrIn[(CH_2)_3NMe_2]_2$ [28] in CH_2Cl_2 was added to 4.68 g (18.2 mmol) $Ag[CF_3SO_3]$ and refluxed for 48 h. After filtration, removing the solvent and resolving the residue in toluene the solution was added by filtration to a suspension of 2.34 g (36 mmol) of dried sodium azide in toluene. The mixture was refluxed for additional 48 h. After filtration the solvent was removed in vacuo remaining a pale brown solid. Analytically pure colorless crystals were obtained after sublimation (100°C, 10^{-3} Torr dynamic vacuum) and recrystallization from CH_2Cl_2/n-pentane at $-35°C$. Yield 3.0 g (9.1 mmol; 75%). Anal. Found: C, 36.02; H, 7.21; N 20.70. $C_{10}H_{24}N_5In$ ($M = 329.15$). Calc.: C, 36.49; H, 7.35; N, 21.28. ^1H NMR (benzene-d_6, 25°C) $\delta = 0.47$ (t, 2H, $InCH_2$); 1.70 (quin, 2H, $-CH_2-$); 2.14 (t, 2H, NCH_2); 2.19 (s, 6H, NCH_3). ^{13}C NMR (benzene-d_6, 25°C): $\delta = 5.7$ ($InCH_2$); 22.8 (CH_2); 43.9 (NCH_3); 61.4 (NCH_2). IR (toluene, CaF_2, cm^{-1}): 2055 vs (N_3, asym.); 1460 s (N_3, sym.).

7.5. Thin film growth

The reactor was kept at 500°C at a basic pressure of 10^{-6} Torr for 5 h loaded it with the cleaned substrates. Then the precursor reservoir was filled with 500 mg of **3** under inert gas atmosphere and cooled down to $-30°C$. The system was pumped down again to 10^{-6} Torr for 1–2 h. During this time the substrates were heated to 100–150°C above the deposition temperature for 30 min (to liberate any condensed material). When GaAs substrates were used the reactor was never heated above 500°C. After this the temperature of the oven was allowed to stabilize at the desired value (350–570°C). The temperature of the bubbler was then adjusted at 70°C allowing **3** to sublime through the hot zone of the reactor at pressures of 0.5×10^{-4} to 2.0×10^{-4} Torr. In the case of carrier gases and flow conditions, the temperature of the bubbler was kept at 90°C at a

Table 2
Summary of crystallographic data for the compounds 1, 2 and 3

	1	2	3
Formula	$C_{15}H_{15}InN_{12}$	$C_{21}H_{48}N_7In_2O_3F_3S$	$C_{10}H_{24}InN_5$
Weight	478.19	765.35	329.15
Space group	$P\bar{1}$	$P2_1/n$	$P\bar{1}$
Crystal system	triclinic	monoclinic	triclinic
a (pm)	900.3(5)	1306.1(2)	652.06(5)
b (pm)	1014.0(5)	1339.4(1)	703.08(8)
c (pm)	1268.3(6)	1863.2(3)	936.03(11)
α (deg)	100.18(2)	90	79.227(10)
β (deg)	102.79(2)	100.70(1)	72.986(8)
γ (deg)	116.07(2)	90	63.643(8)
V (10^6 pm^3)	963.3(3)	3202.8(8)	366.8(7)
Z	2	4	1
d_{calc} (g cm^{-3})	1.649	1.579	1.490
Crystal size (mm)	$0.7 \times 0.25 \times 0.15$	$0.80 \times 0.12 \times 0.12$	$0.38 \times 0.13 \times 0.08$
$\Theta_{min.}-\Theta_{max.}$ (deg)	1.73–32	1.8–26	4.1–25.6
μ (cm^{-1})	12.6	15.3	16.0
Final R	0.0335	0.0308	0.0167
Final Rw	0.0740	0.0758	0.0418
No. of unique reflections	6684	5711	1279
No. of observed reflections	5618	4936	1279

pressure of 7.5×10^{-1} Torr at typical flow rates of 50 sccm (N_2) and 5–10 sccm (NH_3).

7.6. X-ray crystallography

7.6.1. Single crystal studies

The data for 1 were collected on an Siemens Stoe-AED2 four-circle diffractometer using the ω-scan technique and Mo Kα radiation ($\lambda = 71.073$ pm) at $-70°C$. For 2 and 3 the data were collected on a Stoe & Cie IPDS diffractometer with Mo Kα graphite monochromated radiation ($\lambda = 71.073$ pm) at $-50°C$. The structures were solved by direct methods (SHELXS-86 [29]) and for the coordinates and anisotropic thermal parameters of the non-hydrogen atoms, full-matrix least-squares refinements (SHELXL-93 [30]) based on F^2 were carried out. The crystallographic data of 1–3 are summarized in Table 2. Additional crystallographic data for compound 1 reported in this paper has been deposited with the Cambridge Crystallographic Data Centre. Copies of the data can be obtained free of charge on application to The Director, CCDC, 12 Union Road, Cambridge CB2IEZ, UK. Further details on the crystal structure investigations of 2 and 3 can be obtained from the Fachinformationszentrum Karlsruhe, D-76344, Eggenstein-Leopoldshafen upon quoting the following numbers: CSD-406747(2); CSD-406746(3).

7.7. Thin film studies

X-ray diffraction measurements were performed on a Philips PW3040 diffractometer including a PW3020 ω-2Θ two-circle diffractometer equipped with the thin film package and a graphite monochromator. Cu Kα radiation was used. The instrumental resolution in 2Θ-Θ mode is about 0.1° in 2Θ and in the X-ray rocking curve mode about 0.15° in (ω). The samples were mounted on a single crystal sample holder to improve the signal-to-noise ratio. All samples were analyzed by a conventional 2Θ-Θ scan. (JCPDS-ICDD No. 2-1430).

References

[1] D.A. Neumayer, J.G. Ekerdt, Chem. Mater. 8 (1996) 9, and references cited therein.
[2] G.B. Stringfellow, Organometallic Vapor-Phase Epitaxy, Academic Press, New York, 1989.
[3] M.L. Hitchman, K.F. Jensen (Eds.), Chemical Vapor Deposition, Principles and Applications, Academic Press, London, 1993.
[4] O. Ambacher, A. Bergmaier, M.S. Brandt, R. Dimitrov, G. Dollinger, R.A. Fischer, A. Miehr, T. Metzger, M. Stutzmann, J. Vac. Sci. Technol. B 14 (1996), (in press).
[5] a) P. O'Brien, in: D.W. Bruce, D. O'Hare (Eds.), Inorganic Materials, ch. 9, Wiley, New York, 1992, p. 492. b) M.J. Hampden-Smith, T.T. Kodas (Eds.), in: The Chemistry of Metals CVD, Verlag Chemie, Weinheim, 1994. c) R.A. Fischer, Chemie in unserer Zeit, 29 (1995) 141.
[6] E. Wiberg, H. Michaud, Z. Naturforsch. B 9 (1954) 495.
[7] J. Kouvetakis, D. Beach, Chem. Mater. 1 (1989) 476.
[8] D.C. Boyd, R.T. Haasch, D.R. Mantell, R.K. Schulze, J.F. Evans, W.L. Gladfelter, Chem. Mater. 1 (1989) 119.
[9] I.C. Tornieporth-Oetting, T.M. Klapötke, Angew. Chem. 107 (1995) 559, and references cited therein.
[10] H. Bock, R. Dammel, Angew. Chem. 99 (1987) 518, and references cited therein.
[11] a) V. Lakhotia, D.A. Neumayer, A.H. Cowley, R.A. Jones, J.G. Ekerdt, Chem. Mater. 7 (1995) 546. b) D.A. Neumayer, A.H. Cowley, A. Decken, R.A. Jones, V. Lakhotia, J.G. Ekerdt, J. Am. Chem. Soc. 117 (1995) 5893.

[12] A. Miehr, O. Ambacher, Th. Metzger, E. Born, R.A. Fischer, Chem. Vap. Deposit. 2 (1996) 51.

[13] A. Miehr, M.R. Mattner, R.A. Fischer, Organometallics 15 (1996) 2053.

[14] R.A. Fischer, A. Miehr, E. Herdtweck, M.R. Mattner, O. Ambacher, T. Metzger, E. Born, S. Weinkauf, C.R. Pulham, S. Parsons, Chem. Eur. J. 2 (1996) 101.

[15] A. Miehr, O. Ambacher, T. Metzger, E. Born, R.A. Fischer, J. Cryst. Growth 170 (1996) 139.

[16] R.A. Fischer, A. Miehr, H. Sussek, H. Pritzkow, E. Herdtweck, J. Müller, O. Ambacher, T. Metzger, Chem. Commun. (1996) 2685.

[17] R.A. Fischer, A. Miehr, T. Metzger, E. Born, O. Ambacher, H. Angerer, R. Dimitrov, Chem. Mater. 8 (1996) 1356.

[18] H. Sussek, Diploma Thesis, Ruprecht-Karls Universität Heidelberg, 1996.

[19] C.J. Carmalt, A.H. Cowley, R.D. Culp, R.A. Jones, Chem. Commun. (1996) 1453.

[20] H. Schumann, U. Hartmann, W. Wassermann, O. Just, A. Dietrich, L. Pohl, M. Hostalek, M. Lokai, Chem. Ber. 124 (1991) 1113.

[21] a) M. Hostalek, L. Pohl, A. Brauers, P. Balk, V. Frese, H. Hardtdegen, R. Hövel, G.K. Regel, Thin Solid Films 174 (1989) 1. b) V. Frese, G.K. Regel, H. Hardtdegen, A. Brauers, P. Balk, M. Hostalek, M. Lokai, L. Pohl, J. Cryst. Growth 102 (1990) 290.

[22] a) H. Schumann, F.H. Görlitz, T.D. Seuss, W. Wassermann, Chem. Ber. 125 (1992) 3. b) H. Schumann, T.D. Seuss, O. Just, R. Weimann, H. Hemling, F.H. Gorlitz, J. Organomet. Chem. 479 (1994) 171, and references cited therein. c) A.H. Cowley, F.P. Gabbai, H.S. Isom, A. Decken, R. Culp, Main Group Chemistry 1 (1996) 1.

[23] R.A. Fischer, E. Herdtweck, T. Spiegler, A. Miehr, unpublished results 1996/1997. For details contact the authors E.H. and R.A.F.

[24] R.A. Fischer, M. Kleine, M. Stuke, O. Lehmann, Chem. Mater. 7 (1995) 1863.

[25] G. Packeiser, Adv. Mater. 2 (1990) 464.

[26] J.B. MacChesney, P.M. Bridenbaugh, P.B. O'Connor, Mater. Res. Bull. 5 (1970) 783.

[27] B.R. Natarajan, A.H. Eltoukhy, J.E. Greene, T.L. Barr, Thin Solid Films 69 (1980) 217.

[28] H. Schumann, F.H. Görlitz, T.D. Seuss, W. Wassermann, Chem. Ber. 125 (1992) 3–7.

[29] G.M. Sheldrick, SHELXS-86, in: G.M. Sheldrick, C. Krüger, R. Goddard (Eds.), Crystallographic Computing 3, Oxford University Press, UK, 1986, pp. 175–189.

[30] G.M. Sheldrick, SHELXL-93, in: J. Appl. Cryst. (1993).